The Heteronuclear Cluster Chemistry of the Group 1B Metals. Part 9.[1] Stereochemical Non-rigidity of the Metal Skeletons of Cluster Compounds in Solution. ^{109}Ag-{^{1}H} INEPT Nuclear Magnetic Resonance Studies on $[Ag_2Ru_4(\mu_3\text{-}H)_2\{\mu\text{-}Ph_2P(CH_2)_nPPh_2\}(CO)_{12}]$ (n = 1, 2, or 4) and X-Ray Crystal Structure of $[Ag_2Ru_4(\mu_3\text{-}H)_2(\mu\text{-}Ph_2PCH_2PPh_2)(CO)_{12}]$†

Scott S. D. Brown, Ian D. Salter,* and Vladimir Šik
Department of Chemistry, University of Exeter, Exeter EX4 4QD
Ian J. Colquhoun and William McFarlane*
Department of Chemistry, City of London Polytechnic, London EC3N 2EY
Paul A. Bates and Michael B. Hursthouse
Department of Chemistry, Queen Mary College, University of London, London E1 4NS
Martin Murray
Department of Organic Chemistry, University of Bristol, Bristol BS8 1TS

A combination of spectroscopic data and an X-ray diffraction study on $[Ag_2Ru_4(\mu_3\text{-}H)_2(\mu\text{-}Ph_2PCH_2PPh_2)(CO)_{12}]$ [Ag–Ag 2.756(6), Ag–Ru 2.820(6)—3.151(6), Ru–Ru 2.775(7)—2.998(6) Å] shows that the clusters $[Ag_2Ru_4(\mu_3\text{-}H)_2\{\mu\text{-}Ph_2P(CH_2)_nPPh_2\}(CO)_{12}]$ (n = 1—6) all adopt a capped trigonal-bipyramidal metal core geometry. However, although there are two distinct silver sites in the ground-state structures, ambient temperature ^{109}Ag-{^{1}H} INEPT n.m.r. spectra of the clusters in which n = 1, 2, or 4 show a single averaged silver resonance in each case. These studies provide the first direct evidence for stereochemical non-rigidity of the metal skeletons of Group 1B metal heteronuclear clusters in solution. In addition, values of $^1J(^{107,109}Ag\ ^{107,109}Ag)$ have been measured for the first time. The results of ^{31}P-{^{109}Ag} and ^{109}Ag INEPT and DEPT n.m.r. studies on $[AgRu_4(\mu_3\text{-}H)_3(CO)_{12}(PPh_3)]$ are also reported.

Some of us have recently reported the synthesis of the novel bimetallic cluster compounds $[M_2Ru_4(\mu_3\text{-}H)_2\{\mu\text{-}Ph_2P(CH_2)_n\text{-}PPh_2\}(CO)_{12}]$ (M = Cu or Ag; n = 1—6).[2] Single-crystal X-ray diffraction studies on the clusters $[Cu_2Ru_4(\mu_3\text{-}H)_2\text{-}\{\mu\text{-}Ph_2P(CH_2)_nPPh_2\}(CO)_{12}]$ (n = 2, 3, or 5) reveal capped trigonal-bipyramidal metal core structures, with the two copper atoms in close contact. The bidentate diphosphine ligand bridges the two copper atoms, which occupy geometrically distinct sites. Spectroscopic data suggest that the other clusters in the series all adopt the same skeletal geometry.[2]

Although there are two phosphorus environments in the ground-state structures of all of the above clusters, ^{31}P-{^{1}H} and ^{1}H n.m.r. spectra reveal two equivalent phosphorus atoms at ambient temperature.[2] In the absence of any chemically reasonable alternative explanation,[2,3] it has been proposed that the fluxional process occurring is an intramolecular rearrangement of the actual metal skeletons of the clusters. Similar dynamic behaviour has also been postulated for a considerable number of other heteronuclear Group 1B metal cluster compounds which contain two or more inequivalent $M(PR_3)$ (M = Cu, Ag, or Au; R = alkyl or aryl) moieties, but no direct evidence to support these hypotheses has been previously reported.[4]

Both naturally occurring isotopes of silver (^{107}Ag and ^{109}Ag) have $I = \frac{1}{2}$. Thus, in principle, ^{107}Ag or ^{109}Ag n.m.r. spectroscopy could be used to investigate the stereochemical non-rigidity of the metal frameworks of silver cluster compounds in solution. In practice, however, it is extremely difficult to observe n.m.r. signals from ^{107}Ag or ^{109}Ag directly, because of the low magnetogyric ratios (γ values) and long T_1 values of these nuclei.[5] However, spin-polarization transfer techniques such as INEPT[6,7] can provide large gains in sensitivity for nuclei with low γ values, as long as they are coupled to nuclei with high γ values, particularly protons. Previously, ^{109}Ag-{^{1}H} INEPT n.m.r. experiments have only been used to study a few simple silver compounds,[8] but herein we report the first use of the technique to detect silver resonances in cluster compounds. The ^{109}Ag-{^{1}H} INEPT n.m.r. studies on the clusters $[Ag_2Ru_4\text{-}(\mu_3\text{-}H)_2\{\mu\text{-}Ph_2P(CH_2)_nPPh_2\}(CO)_{12}]$ (n = 1, 2, or 4) directly confirm that these species undergo a fluxional process in solution which exchanges the silver atoms between the two distinct coinage metal sites in the ground-state structures. Preliminary accounts describing some of our work have already been published.[9,10]

Results and Discussion

Infrared and n.m.r. spectroscopic data suggest [2] that the clusters $[Ag_2Ru_4(\mu_3\text{-}H)_2\{\mu\text{-}Ph_2P(CH_2)_nPPh_2\}(CO)_{12}]$ [n = 1 (**1**), 2 (**2**), 3 (**3**), 4 (**4**), 5 (**5**), or 6 (**6**)] adopt capped trigonal-bipyramidal metal core structures. A single-crystal X-ray diffraction study on (**1**) now confirms this hypothesis. Discussion of the n.m.r. data is best deferred until the X-ray diffraction results have been described.

Two independent molecules (A and B) are present in the asymmetric unit of (**1**). The molecular structure of (**1**) is illustrated in Figure 1, which also shows the crystallographic numbering. Selected interatomic distances and angles for molecules A and B‡ are summarized in Table 1. The X-ray diffraction study

† 1,2-μ-[Bis(diphenylphosphino)methane]-3,3,3,4,4,4,5,5,5,6,6,6-dodecacarbonyl-1,3,4;1,3,5-di-μ_3-hydrido-*cyclo*-disilvertetraruthenium (*Ag–Ag*, 5*Ag–Ru*, 6*Ru–Ru*).

Supplementary data available: see Instructions for Authors, *J. Chem. Soc., Dalton Trans.*, 1988, Issue 1, pp. xvii—xx.

‡ The differences between the two molecules are marginal, except for the Ag(12)–Ru(13) and Ag(22)–Ru(23) separations, which differ by 0.054 Å, and the Ag(12)–Ru(14) and Ag(22)–Ru(24) separations which differ by 0.046 Å. When the interatomic distances for the two molecules are not significantly different, those quoted in the text are for molecule A.

Table 1. Selected bond lengths (Å) and angles (°), with estimated standard deviations in parentheses, for $[Ag_2Ru_4(\mu_3\text{-}H)_2(\mu\text{-}Ph_2PCH_2PPh_2)(CO)_{12}]$ (**1**)

(*i*) Molecule A[a]

Ag(12)–Ag(11)	2.756(6)	Ru(13)–Ag(11)	2.850(6)		
Ru(14)–Ag(11)	2.823(6)	P(11)–Ag(11)	2.452(10)		
Ru(11)–Ag(12)	2.881(6)	Ru(13)–Ag(12)	3.151(6)		
Ru(14)–Ag(12)	2.958(6)	P(12)–Ag(12)	2.390(10)		
Ru(12)–Ru(11)	2.787(6)	Ru(13)–Ru(11)	2.964(6)		
Ru(14)–Ru(11)	2.998(6)	Ru(13)–Ru(12)	2.786(7)		
Ru(14)–Ru(12)	2.789(6)	Ru(14)–Ru(13)	2.953(6)		
C(1)–P(11)	1.879(29)	C(1A1)–P(11)	1.845(18)		
C(1B1)–P(11)	1.805(18)	C(1)–P(12)	1.790(29)		
C(1C1)–P(12)	1.821(17)	C(1D1)–P(12)	1.818(19)		
Average Ru–C	1.86(2)	Average C–O	1.15(1)		
Ru(13)–Ag(11)–Ag(12)	68.4(2)	Ru(14)–Ag(11)–Ag(12)	64.0(2)		
Ru(14)–Ag(11)–Ru(13)	62.7(2)	P(11)–Ag(11)–Ag(12)	95.4(3)		
P(11)–Ag(11)–Ru(13)	129.5(3)	P(11)–Ag(11)–Ru(14)	152.0(2)		
Ru(11)–Ag(12)–Ag(11)	108.2(2)	Ru(13)–Ag(12)–Ag(11)	57.2(2)		
Ru(13)–Ag(12)–Ru(11)	58.7(2)	Ru(14)–Ag(12)–Ag(11)	59.1(2)		
Ru(14)–Ag(12)–Ru(11)	61.8(2)	Ru(14)–Ag(12)–Ru(13)	57.7(2)		
P(12)–Ag(12)–Ag(11)	92.0(3)	P(12)–Ag(12)–Ru(11)	156.5(2)		
P(12)–Ag(12)–Ru(13)	129.7(3)	P(12)–Ag(12)–Ru(14)	141.6(2)		
Ru(12)–Ru(11)–Ag(12)	110.1(2)	Ru(13)–Ru(11)–Ag(12)	65.2(2)		
Ru(13)–Ru(11)–Ru(12)	57.8(2)	Ru(14)–Ru(11)–Ag(12)	60.4(2)		
Ru(14)–Ru(11)–Ru(12)	57.5(2)	Ru(14)–Ru(11)–Ru(13)	59.4(2)		
C(11)–Ru(11)–Ag(12)	70.7(9)	C(11)–Ru(11)–Ru(12)	178.5(8)		
C(11)–Ru(11)–Ru(13)	122.0(9)	C(11)–Ru(11)–Ru(14)	123.8(9)		
C(12)–Ru(11)–Ag(12)	135.1(11)	C(12)–Ru(11)–Ru(12)	86.7(11)		
C(12)–Ru(11)–Ru(13)	93.8(11)	C(12)–Ru(11)–Ru(14)	142.5(10)		
C(12)–Ru(11)–C(11)	91.9(14)	C(13)–Ru(11)–Ag(12)	131.7(10)		
C(13)–Ru(11)–Ru(12)	83.5(11)	C(13)–Ru(11)–Ru(13)	140.8(10)		
C(13)–Ru(11)–Ru(14)	95.8(12)	C(13)–Ru(11)–C(11)	96.8(14)		
C(13)–Ru(11)–C(12)	90.2(16)	Ru(13)–Ru(12)–Ru(11)	64.3(2)		
Ru(14)–Ru(12)–Ru(11)	65.0(2)	Ru(14)–Ru(12)–Ru(13)	64.0(2)		
C(14)–Ru(12)–Ru(11)	99.5(11)	C(14)–Ru(12)–Ru(13)	97.0(11)		
C(14)–Ru(12)–Ru(14)	159.0(10)	C(15)–Ru(12)–Ru(11)	162.5(11)		
C(15)–Ru(12)–Ru(13)	103.0(12)	C(15)–Ru(12)–Ru(14)	99.1(11)		
C(15)–Ru(12)–C(14)	93.8(15)	C(16)–Ru(12)–Ru(11)	96.1(14)		
C(16)–Ru(12)–Ru(13)	158.2(13)	C(16)–Ru(12)–Ru(14)	100.2(14)		
C(16)–Ru(12)–C(14)	95.4(17)	C(16)–Ru(12)–C(15)	93.9(18)		
Ag(12)–Ru(13)–Ag(11)	54.4(2)	Ru(11)–Ru(13)–Ag(11)	103.6(2)		
Ru(11)–Ru(13)–Ag(12)	56.1(2)	Ru(12)–Ru(13)–Ag(11)	113.6(2)		
Ru(12)–Ru(13)–Ag(12)	102.9(2)	Ru(12)–Ru(13)–Ru(11)	57.9(2)		
Ru(14)–Ru(13)–Ag(11)	58.2(2)	Ru(14)–Ru(13)–Ag(12)	57.9(2)		
Ru(14)–Ru(13)–Ru(11)	60.9(2)	Ru(14)–Ru(13)–Ru(12)	58.1(2)		
C(17)–Ru(13)–Ag(11)	82.4(12)	C(17)–Ru(13)–Ag(12)	135.9(11)		
C(17)–Ru(13)–Ru(11)	142.2(11)	C(17)–Ru(13)–Ru(12)	85.3(12)		
C(17)–Ru(13)–Ru(14)	94.1(12)	C(18)–Ru(13)–Ag(11)	65.7(10)		
C(18)–Ru(13)–Ag(12)	75.6(10)	C(18)–Ru(13)–Ru(11)	120.8(10)		
C(18)–Ru(13)–Ru(12)	178.5(9)	C(18)–Ru(13)–Ru(14)	120.8(10)		
C(18)–Ru(13)–C(17)	95.9(15)	C(19)–Ru(13)–Ag(11)	156.1(11)		
C(19)–Ru(13)–Ag(12)	131.9(10)	C(19)–Ru(13)–Ru(11)	95.7(11)		
C(19)–Ru(13)–Ru(12)	88.5(12)	C(19)–Ru(13)–Ru(14)	145.5(11)		
C(19)–Ru(13)–C(17)	91.0(16)	C(19)–Ru(13)–C(18)	92.5(15)		
Ag(12)–Ru(14)–Ag(11)	56.9(2)	Ru(11)–Ru(14)–Ag(11)	103.4(2)		
Ru(11)–Ru(14)–Ag(12)	57.9(2)	Ru(12)–Ru(14)–Ag(11)	114.3(2)		
Ru(12)–Ru(14)–Ag(12)	107.9(2)	Ru(12)–Ru(14)–Ru(11)	57.5(2)		
Ru(13)–Ru(14)–Ag(11)	59.1(2)	Ru(13)–Ru(14)–Ag(12)	64.4(2)		
Ru(13)–Ru(14)–Ru(11)	59.7(2)	Ru(13)–Ru(14)–Ru(12)	58.0(2)		
C(110)–Ru(14)–Ag(11)	79.5(9)	C(110)–Ru(14)–Ag(12)	136.3(8)		
C(110)–Ru(14)–Ru(11)	141.1(8)	C(110)–Ru(14)–Ru(12)	85.6(9)		
C(110)–Ru(14)–Ru(13)	91.8(9)	C(111)–Ru(14)–Ag(11)	72.1(10)		
C(111)–Ru(14)–Ag(12)	75.8(10)	C(111)–Ru(14)–Ru(11)	122.8(10)		
C(111)–Ru(14)–Ru(12)	173.6(9)	C(111)–Ru(14)–Ru(13)	128.3(10)		
C(111)–Ru(14)–C(110)	95.3(13)	C(112)–Ru(14)–Ag(11)	162.0(10)		
C(112)–Ru(14)–Ag(12)	128.6(11)	C(112)–Ru(14)–Ru(11)	92.3(11)		
C(112)–Ru(14)–Ru(12)	81.5(11)	C(112)–Ru(14)–Ru(13)	138.5(10)		
C(112)–Ru(14)–C(110)	93.9(13)	C(112)–Ru(14)–C(111)	92.1(14)		
C(1A1)–P(11)–Ag(11)	116.6(8)	C(1B1)–P(11)–Ag(11)	117.4(8)		
C(1B1)–P(11)–C(1A1)	105.9(10)	C(1)–P(11)–Ag(11)	108.1(11)		
C(1)–P(11)–C(1A1)	103.5(12)	C(1)–P(11)–C(1B1)	103.6(12)		
C(1C1)–P(12)–Ag(12)	116.9(8)	C(1D1)–P(12)–Ag(12)	115.3(8)		

(*ii*) Molecule B[b]

Ag(22)–Ag(21)	2.756(6)	Ru(23)–Ag(21)	2.844(6)		
Ru(24)–Ag(21)	2.820(6)	P(21)–Ag(21)	2.436(10)		
Ru(21)–Ag(22)	2.894(6)	Ru(23)–Ag(22)	3.097(6)		
Ru(24)–Ag(22)	3.004(6)	P(22)–Ag(22)	2.412(10)		
Ru(22)–Ru(21)	2.800(7)	Ru(23)–Ru(21)	2.982(6)		
Ru(24)–Ru(21)	2.987(6)	Ru(23)–Ru(22)	2.775(7)		
Ru(24)–Ru(22)	2.797(6)	Ru(24)–Ru(23)	2.941(6)		
C(2)–P(21)	1.832(28)	C(2A1)–P(21)	1.805(18)		
C(2B1)–P(21)	1.832(18)	C(2)–P(22)	1.815(29)		
C(2C1)–P(22)	1.836(20)	C(2D1)–P(22)	1.798(18)		
Average Ru–C	1.86(1)	Average C–O	1.17(1)		
Ru(23)–Ag(21)–Ag(22)	67.1(2)	Ru(24)–Ag(21)–Ag(22)	65.2(2)		
Ru(24)–Ag(21)–Ru(23)	62.6(2)	P(21)–Ag(21)–Ag(22)	96.2(3)		
P(21)–Ag(21)–Ru(23)	128.8(3)	P(21)–Ag(21)–Ru(24)	154.1(2)		
Ru(21)–Ag(22)–Ag(21)	108.3(2)	Ru(23)–Ag(22)–Ag(21)	57.8(2)		
Ru(23)–Ag(22)–Ru(21)	59.6(2)	Ru(24)–Ag(22)–Ag(21)	58.4(2)		
Ru(24)–Ag(22)–Ru(21)	60.8(2)	Ru(24)–Ag(22)–Ru(23)	57.6(2)		
P(22)–Ag(22)–Ag(21)	91.1(3)	P(22)–Ag(22)–Ru(21)	158.8(2)		
P(22)–Ag(22)–Ru(23)	129.9(3)	P(22)–Ag(22)–Ru(24)	139.9(2)		
Ru(22)–Ru(21)–Ag(22)	109.8(2)	Ru(23)–Ru(21)–Ag(22)	63.6(2)		
Ru(23)–Ru(21)–Ru(22)	57.3(2)	Ru(24)–Ru(21)–Ag(22)	61.4(2)		
Ru(24)–Ru(21)–Ru(22)	57.7(2)	Ru(24)–Ru(21)–Ru(23)	59.0(2)		
C(21)–Ru(21)–Ag(22)	69.7(11)	C(21)–Ru(21)–Ru(22)	175.1(9)		
C(21)–Ru(21)–Ru(23)	125.1(11)	C(21)–Ru(21)–Ru(24)	119.0(10)		
C(22)–Ru(21)–Ag(22)	133.2(11)	C(22)–Ru(21)–Ru(22)	85.4(11)		
C(22)–Ru(21)–Ru(23)	93.3(11)	C(22)–Ru(21)–Ru(24)	141.5(10)		
C(22)–Ru(21)–C(21)	98.5(15)	C(23)–Ru(21)–Ag(22)	132.9(10)		
C(23)–Ru(21)–Ru(22)	82.1(12)	C(23)–Ru(21)–Ru(23)	138.3(11)		
C(23)–Ru(21)–Ru(24)	93.2(12)	C(23)–Ru(21)–C(21)	94.8(16)		
C(23)–Ru(21)–C(22)	91.9(16)	Ru(23)–Ru(22)–Ru(21)	64.7(2)		
Ru(24)–Ru(22)–Ru(21)	64.5(2)	Ru(24)–Ru(22)–Ru(23)	63.7(2)		
C(24)–Ru(22)–Ru(21)	100.0(11)	C(24)–Ru(22)–Ru(23)	102.7(11)		
C(24)–Ru(22)–Ru(24)	162.3(10)	C(25)–Ru(22)–Ru(21)	161.8(10)		
C(25)–Ru(22)–Ru(23)	97.9(11)	C(25)–Ru(22)–Ru(24)	103.9(10)		
C(25)–Ru(22)–C(24)	88.7(14)	C(26)–Ru(22)–Ru(21)	96.8(16)		
C(26)–Ru(22)–Ru(23)	158.0(14)	C(26)–Ru(22)–Ru(24)	98.3(15)		
C(26)–Ru(22)–C(24)	91.8(18)	C(26)–Ru(22)–C(25)	98.9(19)		
Ag(22)–Ru(23)–Ag(21)	55.1(2)	Ru(21)–Ru(23)–Ag(21)	103.7(2)		
Ru(21)–Ru(23)–Ag(22)	56.8(2)	Ru(22)–Ru(23)–Ag(21)	113.9(2)		
Ru(22)–Ru(23)–Ag(22)	104.8(2)	Ru(22)–Ru(23)–Ru(21)	58.1(2)		
Ru(24)–Ru(23)–Ag(21)	58.3(2)	Ru(24)–Ru(23)–Ag(22)	59.6(2)		
Ru(24)–Ru(23)–Ru(21)	60.6(2)	Ru(24)–Ru(23)–Ru(22)	58.5(2)		
C(27)–Ru(23)–Ag(21)	79.0(10)	C(27)–Ru(23)–Ag(22)	133.8(9)		
C(27)–Ru(23)–Ru(21)	144.1(10)	C(27)–Ru(23)–Ru(22)	87.7(11)		
C(27)–Ru(23)–Ru(24)	93.8(11)	C(28)–Ru(23)–Ag(21)	68.5(10)		
C(28)–Ru(23)–Ag(22)	73.1(10)	C(28)–Ru(23)–Ru(21)	117.9(10)		
C(28)–Ru(23)–Ru(22)	175.4(9)	C(28)–Ru(23)–Ru(24)	122.3(10)		
C(28)–Ru(23)–C(27)	96.6(15)	C(29)–Ru(23)–Ag(21)	159.5(10)		
C(29)–Ru(23)–Ag(22)	130.4(10)	C(29)–Ru(23)–Ru(21)	93.1(11)		
C(29)–Ru(23)–Ru(22)	84.9(11)	C(29)–Ru(23)–Ru(24)	142.0(10)		
C(29)–Ru(23)–C(27)	94.3(14)	C(29)–Ru(23)–C(28)	93.4(14)		
Ag(22)–Ru(24)–Ag(21)	56.4(2)	Ru(21)–Ru(24)–Ag(21)	104.2(2)		
Ru(21)–Ru(24)–Ag(22)	57.8(2)	Ru(22)–Ru(24)–Ag(21)	114.0(2)		
Ru(22)–Ru(24)–Ag(22)	106.8(2)	Ru(22)–Ru(24)–Ru(21)	57.8(2)		
Ru(23)–Ru(24)–Ag(21)	59.1(2)	Ru(23)–Ru(24)–Ag(22)	62.8(2)		
Ru(23)–Ru(24)–Ru(21)	60.4(2)	Ru(23)–Ru(24)–Ru(22)	57.8(2)		
C(210)–Ru(24)–Ag(21)	79.7(10)	C(210)–Ru(24)–Ag(22)	135.2(9)		
C(210)–Ru(24)–Ru(21)	137.4(8)	C(210)–Ru(24)–Ru(22)	81.5(9)		
C(210)–Ru(24)–Ru(23)	88.6(10)	C(211)–Ru(24)–Ag(21)	68.1(10)		
C(211)–Ru(24)–Ag(22)	78.0(10)	C(211)–Ru(24)–Ru(21)	126.4(10)		
C(211)–Ru(24)–Ru(22)	175.2(9)	C(211)–Ru(24)–Ru(23)	125.5(10)		
C(211)–Ru(24)–C(210)	94.9(13)	C(212)–Ru(24)–Ag(21)	159.5(9)		
C(212)–Ru(24)–Ag(22)	127.4(10)	C(212)–Ru(24)–Ru(21)	92.2(10)		
C(212)–Ru(24)–Ru(22)	85.0(10)	C(212)–Ru(24)–Ru(23)	141.3(9)		
C(212)–Ru(24)–C(210)	96.7(14)	C(212)–Ru(24)–C(211)	92.4(14)		
C(2A1)–P(21)–Ag(21)	113.9(8)	C(2B1)–P(21)–Ag(21)	117.3(8)		
C(2B1)–P(21)–C(2A1)	107.4(11)	C(2)–P(21)–Ag(21)	108.5(10)		
C(2)–P(21)–C(2A1)	102.6(12)	C(2)–P(21)–C(2B1)	105.7(12)		
C(2C1)–P(22)–Ag(22)	117.2(9)	C(2D1)–P(22)–Ag(22)	115.3(9)		

Table 1 (*continued*)

(*i*) Molecule A[a]				(*ii*) Molecule B[b]			
C(1D1)–P(12)–C(1C1)	102.8(10)	C(1)–P(12)–Ag(12)	111.9(11)	C(2D1)–P(22)–C(2C1)	102.8(11)	C(2)–P(22)–Ag(22)	111.0(10)
C(1)–P(12)–C(1C1)	104.3(13)	C(1)–P(12)–C(1D1)	104.3(13)	C(2)–P(22)–C(2C1)	105.0(13)	C(2)–P(22)–C(2D1)	104.1(12)
P(12)–C(1)–P(11)	114.4(16)	C(1A2)–C(1A1)–P(11)	124.3(8)	P(22)–C(2)–P(21)	115.6(16)	C(2A2)–C(2A1)–P(21)	116.5(8)
C(1A6)–C(1A1)–P(11)	115.4(8)	C(1B2)–C(1B1)–P(11)	116.0(8)	C(2A6)–C(2A1)–P(21)	123.4(8)	C(2B2)–C(2B1)–P(21)	120.4(8)
C(1B6)–C(1B1)–P(11)	124.0(8)	C(1C2)–C(1C1)–P(12)	122.1(7)	C(2B6)–C(2B1)–P(21)	119.3(8)	C(2C2)–C(2C1)–P(22)	123.6(9)
C(1C6)–C(1C1)–P(12)	117.9(7)	C(1D2)–C(1D1)–P(12)	115.3(8)	C(2C6)–C(2C1)–P(22)	116.3(9)	C(2D2)–C(2D1)–P(22)	118.5(8)
C(1D6)–C(1D1)–P(12)	124.7(8)			C(2D6)–C(2D1)–P(22)	121.5(8)		
Average Ru–C–O	173.3(1)			Average Ru–C–O	171.6(2)		

[a] Phenyl rings '1A' and '1B' are attached to P(11), and '1C' and '1D' to P(12). Each ring is numbered in cyclic order from the α-carbon. [b] Phenyl rings of molecule B are similarly labelled to those of A (the first digit of each number is changed from 1 to 2).

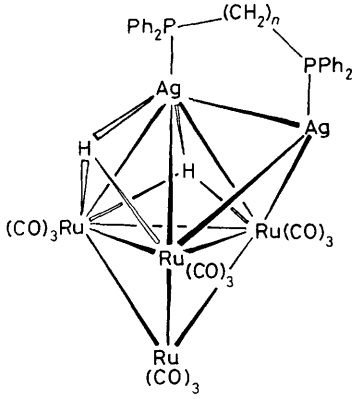

	n
(1)	1
(2)	2
(3)	3
(4)	4
(5)	5
(6)	6

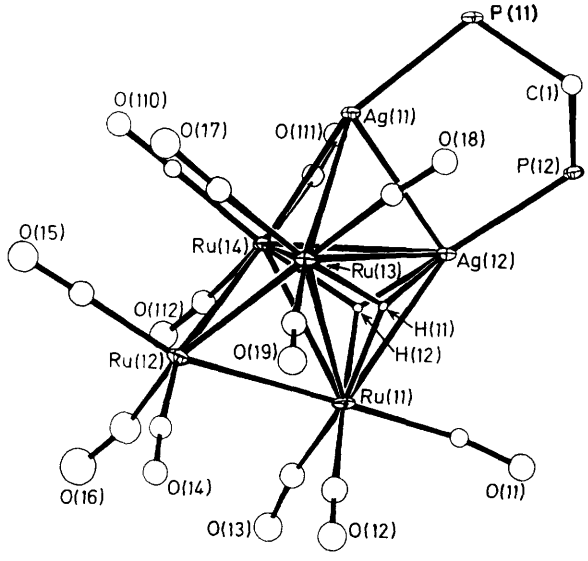

Figure 1. Molecular structure of $[Ag_2Ru_4(\mu_3\text{-}H)_2(\mu\text{-}Ph_2PCH_2PPh_2)(CO)_{12}]$ (**1**), molecule A, showing the crystallographic numbering. For molecule B, the first digit of each number is changed from 1 to 2, except for C(1) in molecule A, which is equivalent to C(2). The phenyl groups have been omitted for clarity and the carbon atom of each carbonyl group has the same number as the oxygen atom

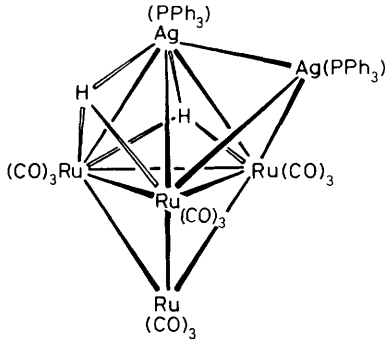

(7)

confirms that the structure deduced by spectroscopic methods is correct. The cluster adopts a capped trigonal-bipyramidal metal core geometry, consisting of a tetrahedron of ruthenium atoms, with one face [Ru(11)Ru(13)Ru(14)] capped by a silver atom [Ag(12)] and one of the faces [Ag(12)Ru(13)Ru(14)] of the $AgRu_3$ tetrahedron so formed further capped by a second silver atom [Ag(11)]. The $Ph_2PCH_2PPh_2$ ligand bridges the Ag(11)–Ag(12) vector, both the Ag(12)Ru(11)Ru(13) and the Ag(12)Ru(11)Ru(14) faces of the metal skeleton are capped by a triply-bridging hydrido ligand, and the Ru atoms are all ligated by three terminal CO groups, which are essentially linear.

The structure of (**1**) is very similar to that established for the analogous PPh_3-containing cluster $[Ag_2Ru_4(\mu_3\text{-}H)_2(CO)_{12}(PPh_3)_2]$ (**7**).[3] The change in ligands attached to the silver atoms from two PPh_3 groups to a $Ph_2PCH_2PPh_2$ ligand shortens the Ag–Ag separation by *ca.* 0.1 Å and lengthens the Ag(12)–Ru(11) vector by *ca.* 0.09 Å. The Ag(*n*2)–Ru(*n*3) and Ag(*n*2)–Ru(*n*4) distances are also considerably lengthened by the change to the bidentate diphosphine [*ca.* 0.27 and 0.05 Å for $n = 1$ and *ca.* 0.22 and 0.09 Å for $n = 2$], but the other metal–metal separations within the capped trigonal-bipyramidal cluster framework are not significantly altered.

The metal–carbonyl angles in (**1**) (179.1—165.8°) are in the normal range observed for terminal CO ligands. In addition, the CO ligands in molecule B exhibit three short Ag–C contacts [Ag(21)–C(28) 2.779(32), Ag(21)–C(211) 2.748(32), and Ag(22)–C(21) 2.849(35) Å] and those in molecule A have one such contact [Ag(11)–C(18) 2.687(33) Å]. Although short M–C contacts between Cu atoms[2,11–14] or Au atoms[13–20] and essentially linear CO ligands bonded to adjacent metals are often observed in heteronuclear clusters, this is the first example of such behaviour in mixed-metal silver clusters.

As the hydrido ligands in (**1**)—(**6**) show coupling to both silver atoms at ambient temperature,[2] $^{109}Ag\text{-}\{^1H\}$ INEPT n.m.r. spectroscopy can be utilized to observe the behaviour of the metal skeletons of these clusters directly. Spectra were measured for (**1**), (**2**), and (**4**), but they are complicated by a

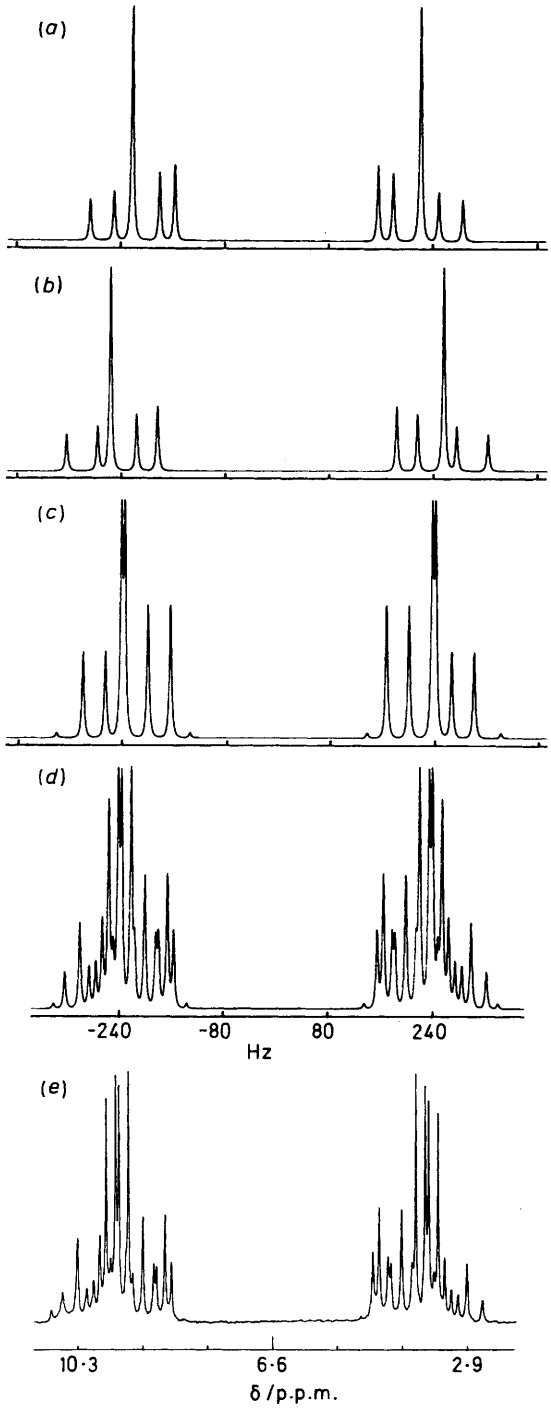

Figure 2. Observed and simulated ^{31}P-$\{^1H\}$ n.m.r. spectra for $[Ag_2Ru_4(\mu_3\text{-}H)_2(\mu\text{-}Ph_2PCH_2PPh_2)(CO)_{12}]$ (**1**). (*a*) Simulated subspectrum for the $^{107}Ag^{107}Ag$ isotopomer (AA′XX′ spin system; 26.9% abundance), (*b*) simulated subspectrum for the $^{109}Ag^{109}Ag$ isotopomer (AA′XX′ spin system; 23.2% abundance), (*c*) simulated subspectrum for the $^{107}Ag^{109}Ag$ isotopomer (AA′MX spin system; 49.9% abundance), (*d*) simulated total spectrum, and (*e*) observed spectrum

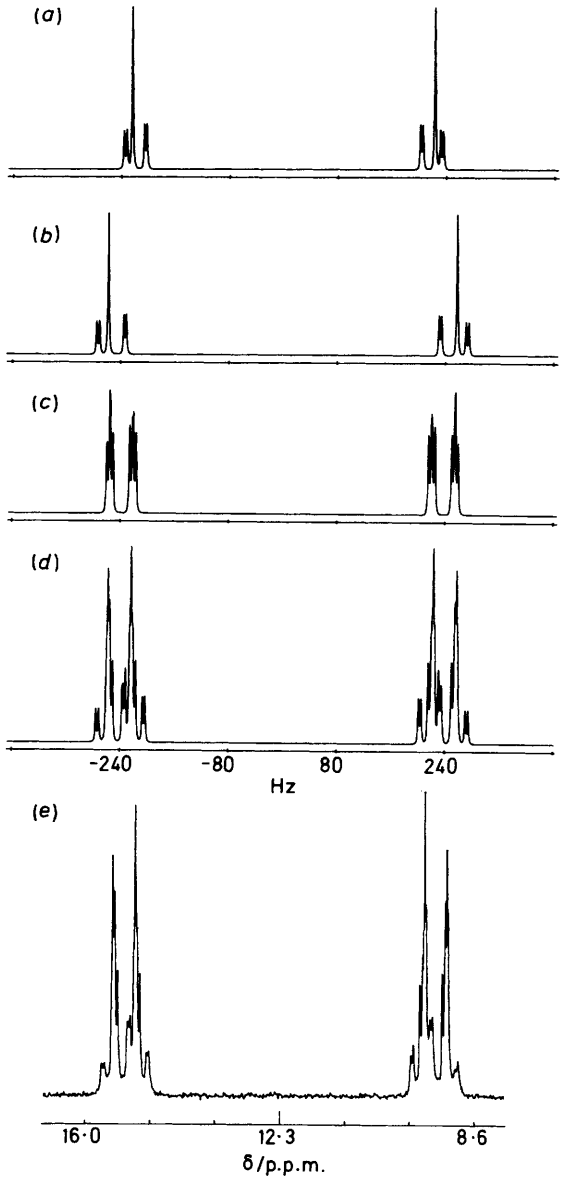

Figure 3. Observed and simulated ^{31}P-$\{^1H\}$ n.m.r. spectra for $[Ag_2Ru_4(\mu_3\text{-}H)_2\{\mu\text{-}Ph_2P(CH_2)_2PPh_2\}(CO)_{12}]$ (**2**). (*a*) Simulated subspectrum for the $^{107}Ag^{107}Ag$ isotopomer (AA′XX′ spin system; 26.9% abundance), (*b*) simulated subspectrum for the $^{109}Ag^{109}Ag$ isotopomer (AA′XX′ spin system; 23.2% abundance), (*c*) simulated subspectrum for the $^{107}Ag^{109}Ag$ isotopomer (AA′MX′ spin system; 49.9% abundance), (*d*) simulated total spectrum, and (*e*) observed spectrum

number of factors. First, three different isotopomers of each cluster are possible from the various combinations of silver isotopes, although ^{109}Ag-$\{^1H\}$ INEPT n.m.r. spectroscopy is only able to observe the $^{107}Ag^{109}Ag$ (49.9%) and the $^{109}Ag^{109}Ag$ (23.2%) isotopomers. Secondly, the INEPT pulse sequence often distorts the relative intensities of the peaks in a spectrum and not all of the expected lines are always observed.[21] Thirdly, the subspectrum due to each isotopomer exhibits a considerable number of couplings and, in most cases, is further complicated by second-order effects. However, the interpretation of the ^{109}Ag-$\{^1H\}$ INEPT n.m.r. spectra is greatly facilitated by the fact that all the values of the relevant coupling constants can be obtained from analysis of the observed ^{31}P-$\{^1H\}$ n.m.r. spectra.

The ambient temperature ^{31}P-$\{^1H\}$ n.m.r. spectra of (**1**)—(**6**) are also complicated by the number of possible isotopomers and by second-order effects. However, the distortions in the relative intensities of the lines associated with the INEPT pulse

Table 2. Ambient temperature ^{109}Ag-{^{1}H} INEPT and ^{31}P-{^{1}H} n.m.r. data[a] for the cluster compounds $[Ag_2Ru_4(\mu_3\text{-}H)_2\{\mu\text{-}Ph_2P(CH_2)_nPPh_2\}(CO)_{12}]$ (n = 1—6)

Compound	Nucleus observed	Chemical shift/δ	$^1J(^{109}AgP)$	$^1J(^{107}AgP)$	$^2J(^{109}AgP)$	$^2J(^{107}AgP)$	$J(PP)$	$^1J(^{109}Ag^{109}Ag)$	$^1J(^{109}Ag^{107}Ag)$	$^1J(^{107}Ag^{107}Ag)$
(1)	^{109}Ag	−153	500[b,c]	—	13[b]	—	—	—	35	—
	^{31}P	6.7	498.5	432.0	12.9	10.4	100.2	40.3	35.0[d]	30.4
(2)	^{109}Ag	−135	510	—	6	—	—	—	35	—
	^{31}P	12.9	510.5	441.7	5.6	5.1	4.2	40.3	35.0[d]	30.4
(3)	^{31}P	15.8	520.5	450.2	7.8	6.8	2.9	44.1	38.2[d]	33.2[d]
(4)	^{109}Ag	−181	523	—	9[c]	—	—	—	41	—
	^{31}P	9.5	523.8	452.3	8.6	7.5	0.0	44.5	38.7[d]	33.7
(5)	^{31}P	6.4	517.2	446.6	10.4	9.0	0.0	46.6	40.5[d]	35.2
(6)	^{31}P	14.0	518.0	448.6	11.5	10.0	1.0	48.4	42.0[d]	36.5

[a] Chemical shifts (δ) in p.p.m., coupling constants in Hz. ^{109}Ag-{^{1}H} INEPT n.m.r. spectra measured in CH_2Cl_2 solution and chemical shifts are positive to high frequency of $[Ag\{P(OEt)_3\}_4]NO_3$ (external). ^{31}P-{^{1}H} N.m.r. spectra measured in [$^2H_2$]dichloromethane–CH_2Cl_2 solution and chemical shifts are positive to high frequency of 85% H_3PO_4 (external). [b] Only the sum of $^1J(^{109}AgP)$ and $^2J(^{109}AgP)$ can be measured from the observed spectra, so the value of $^1J(^{109}AgP)$ has been calculated on the assumption that $^2J(^{109}AgP)$ is 13 Hz, as obtained from the ^{31}P-{^{1}H} n.m.r. spectrum. [c] Mean value of the coupling constants obtained from each of the two separate subspectra. [d] The value of $^1J(^{109}Ag^{107}Ag)$ cannot be measured directly from the ^{31}P-{^{1}H} n.m.r. spectrum, but it can be obtained by calculation from the observed values of $^1J(^{109}Ag^{109}Ag)$ and $^1J(^{107}Ag^{107}Ag)$.

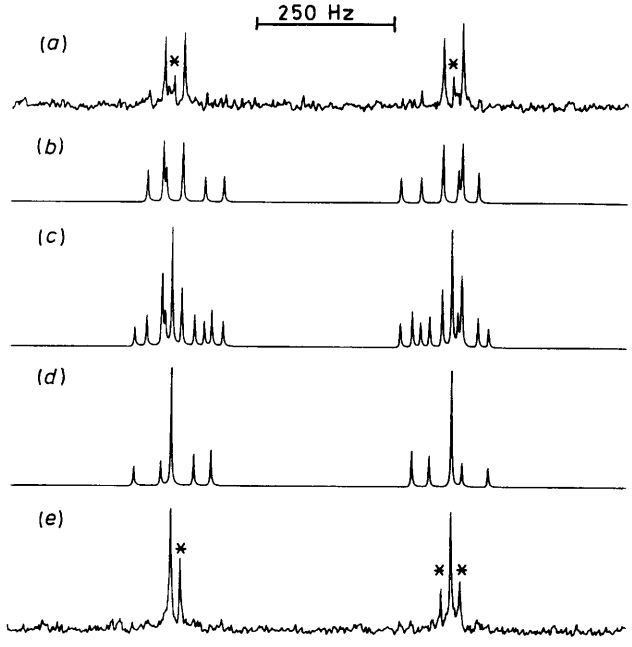

Figure 4. Observed and simulated ^{109}Ag-{^{1}H} n.m.r. spectra for $[Ag_2Ru_4(\mu_3\text{-}H)_2(\mu\text{-}Ph_2PCH_2PPh_2)(CO)_{12}]$ (**1**). (*a*) Observed spectrum with the INEPT timings optimized for the $^{107}Ag^{109}Ag$ isotopomer, (*b*) simulated subspectrum for the $^{107}Ag^{109}Ag$ isotopomer, (*c*) simulated total spectrum, (*d*) simulated subspectrum for the $^{109}Ag^{109}Ag$ isotopomer, and (*e*) observed spectrum with the INEPT timings optimized for the $^{109}Ag^{109}Ag$ isotopomer. For both observed spectra, the vestigial peaks due to the other possible isotopomer are marked by an asterisk

sequence do not occur. The total spectrum of each cluster consists of three superimposed subspectra (Figures 2 and 3). Those due to the $^{107}Ag^{107}Ag$ and $^{109}Ag^{109}Ag$ isotopomers of (**1**)—(**6**) are split by ^{107}Ag–^{31}P or ^{109}Ag–^{31}P couplings through one and two bonds, ^{107}Ag–^{107}Ag or ^{109}Ag–^{109}Ag coupling, and, in some cases, by ^{31}P–^{31}P coupling through the methylene backbone of the bidentate diphosphine ligand and they can be simulated using the A part of an AA′XX′ spin system [Figures 2(*a*), 2(*b*), 3(*a*), and 3(*b*)]. The subspectra due to the $^{107}Ag^{109}Ag$ isotopomers of (**1**)—(**6**) are also split by ^{107}Ag–^{31}P and ^{109}Ag–^{31}P couplings and, in some cases, by ^{31}P–^{31}P coupling, and they can be simulated using the A part of an AA′MX spin system [Figures 2(*c*) and 3(*c*)]. When the three subspectra are all summed together, with the appropriate statistical weightings for the relative isotopic abundances, good fits with the observed spectra are obtained [Figures 2(*d*), 2(*e*), 3(*d*), and 3(*e*)]. The values of the coupling constants obtained from the analyses are presented in Table 2.

To aid the interpretation of the observed ^{109}Ag-{^{1}H} INEPT n.m.r. spectra, the expected form of the two ^{109}Ag-{^{1}H} subspectra of (**1**), (**2**), and (**4**) were calculated using the values of the coupling constants obtained from the analysis of the ^{31}P-{^{1}H} n.m.r. spectra of the clusters. The special features of the spin systems in these silver species allow the INEPT timings for (**1**) to be modified to produce spectra in which the signals due to either the $^{109}Ag^{109}Ag$ or the $^{107}Ag^{109}Ag$ isotopomer are predominant and those from the other species appear only as vestigial peaks (Figure 4). In the normal INEPT pulse sequence,[6,7] shown below, the time interval t is normally set

$$^1H: 90_x° - t - 180° - t - 90_y° - \Delta - 180° - \Delta - \text{Decouple}$$

$$X: \qquad 180° \qquad 90° \qquad 180° \qquad \text{Acquire}$$

equal to $(4J)^{-1}$ for systems in which the spin-polarization transfer occurs within a (XH_n) sub-unit ($I_X = \frac{1}{2}$). With this choice, the proton vectors are 90° out of phase at the time of the first refocussing pulse, and 180° out of phase when the $90_y°$ proton pulse is applied, so that the required transfer of polarization occurs. However, in the case of a (X_2H_n) sub-unit, the proton vectors corresponding to the extreme spin states of X are precessing at twice the normal rate and this value of t would lead to their being 360° out of phase (*i.e.* in phase) at the time of the $90_y°$ pulse. Therefore, there would be no transfer of magnetization. Thus, to achieve the desired result, t must be set equal to $(8J)^{-1}$ in this case, which is, of course, that appertaining to the system with two ^{109}Ag (or ^{107}Ag) nuclei. Under these circumstances, the proton vectors of the (XH_n) sub-unit (*i.e.* a system containing one ^{107}Ag and one ^{109}Ag) will have precessed through 45° and 90° by the times of the 180° and $90_y°$ proton pulses, respectively, and thus there will be out-of-phase *components* along the $\pm x$ axis available to effect a degree of polarization transfer. It is these components that account for the vestigial peaks in Figure 4(*e*). There are also much weaker vestigial peaks from the 'wrong' isotopomer in Figure 4(*a*) and

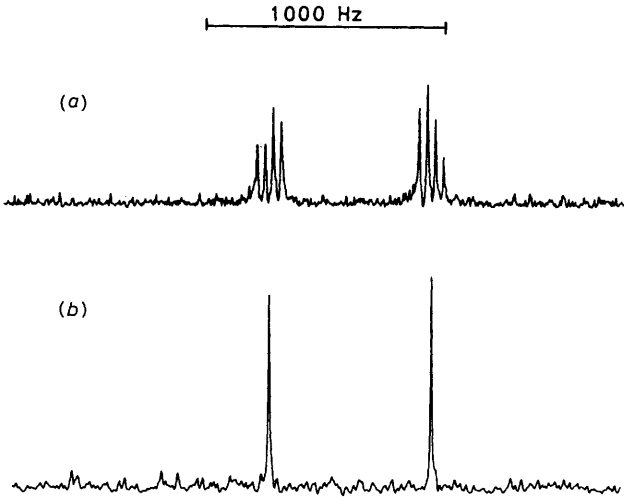

Figure 5. ^{109}Ag INEPT spectra at 4.17 MHz of $[AgRu_4(\mu_3\text{-}H)_3(CO)_{12}(PPh_3)]$ (**8**) in CD_2Cl_2 at −30 °C. (*a*) Recorded using no refocussing or decoupling and in absolute value display mode, and (*b*) recorded using the full refocussed INEPT sequence to achieve proton decoupling during acquisition

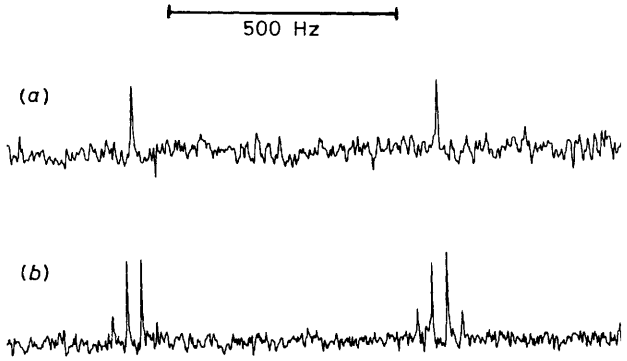

Figure 6. ^{109}Ag DEPT spectra recorded on the same sample as in Figure 5. (*a*) Recorded with proton decoupling, and (*b*) recorded without proton decoupling. Note loss of intensity due to the need for a further refocussing period

they can be attributed to slight mis-settings of the proton pulse lengths and/or r.f. field inhomogeneity. Note that the time interval Δ depends upon the number of *protons* and is therefore unaffected by the foregoing considerations, which, however, would also apply to system in which $I_X > \frac{1}{2}$ (*i.e.* quadrupolar nuclei).

Only a single silver environment is visible in each observed subspectrum for (**1**) (Figure 4). Although by no means all of the expected lines are observed for either isotopomer, perhaps because the values of $J(^{109}AgH)$ and $J(PH)$ are not sufficiently dissimilar, the peaks that are visible all occur in the positions predicted. Indeed, there is an excellent agreement between the values of the coupling constants obtained from the $^{31}P\text{-}\{^1H\}$ n.m.r. spectra and those observed in the $^{109}Ag\text{-}\{^1H\}$ INEPT n.m.r. spectra (Table 2).

The observed $^{109}Ag\text{-}\{^1H\}$ INEPT n.m.r. spectra of (**2**) and (**4**) also closely resemble the calculated spectra, although, as for (**1**), not all of the expected peaks are visible. Again, only a single silver resonance is observed for each cluster. For (**2**), the INEPT timings can be optimized to produce the subspectrum due to the $^{107}Ag^{109}Ag$ isotopomer, but it was not possible to detect the peaks of the $^{109}Ag^{109}Ag$ isotopomer, probably because of the poor solubility of the cluster, together with the fact that the latter isotopomer is only half as abundant as the former. In the case of (**4**), the observed spectrum consists of lines from both isotopomers. Again, the coupling constants obtained from the

Table 3. ^{109}Ag INEPT and DEPT and $^{31}P\text{-}\{^{109}Ag\}$ n.m.r. studies on $[AgRu_4(\mu_3\text{-}H)_3(CO)_{12}(PPh_3)]$ (**8**)

N.m.r. technique used	Chemical shift[a] (δ/p.p.m.)	$J(^{109}AgP)$[b]/Hz	$J(^{109}AgH)$[c]/Hz
^{109}Ag INEPT[d]	−250.4	678	34
^{109}Ag DEPT[d]	−250.4	677	34
$^{31}P\text{-}\{^{109}Ag\}$[e]	−246.4	679	*ca.* 34

[a] Chemical shifts are positive to high frequency of external $[Ag\{P(OEt)_3\}_4]NO_3$. [b] A $J(^{109}AgP)$ value of 693 Hz was measured at −90 °C by $^{31}P\text{-}\{^1H\}$ n.m.r. spectroscopy.[11] [c] A $J(^{109}AgH)$ value of 35 Hz was measured at −80 °C by ^1H n.m.r. spectroscopy.[11] [d] Measured at −30 °C in CD_2Cl_2. [e] Measured at −80 °C in CD_2Cl_2.

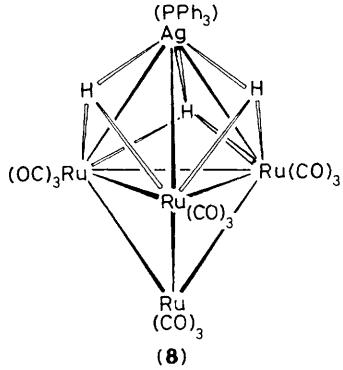

(**8**)

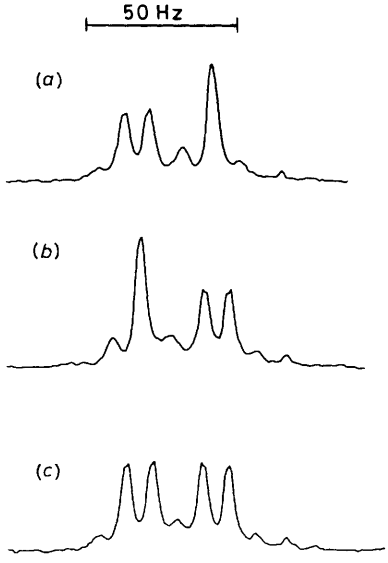

Figure 7. The high-field hydrido ligand resonance in the ^1H n.m.r. spectrum of $[AgRu_4(\mu_3\text{-}H)_3(CO)_{12}(PPh_3)]$ (**8**) in CD_2Cl_2 at −50 °C, with the phenyl protons decoupled. (*a*) With the low-frequency half of the ^{31}P spectrum (corresponding to one spin state of ^{107}Ag or ^{109}Ag) decoupled, (*b*) with the high-frequency half of the ^{31}P spectrum (corresponding to the other spin state of ^{107}Ag or ^{109}Ag) decoupled, and (*c*) normal spectrum. The additional weak peaks are caused by residual effects from the phenyl proton decoupling process. Reduced decoupling power had to be used to avoid affecting the hydrido ligands

Table 4. Atomic positional parameters (fractional co-ordinates) ($\times 10^4$) for $[Ag_2Ru_4(\mu_3\text{-}H)_2(\mu\text{-}Ph_2PCH_2PPh_2)(CO)_{12}]$ (**1**), with estimated standard deviations in parentheses

Atom	*x*	*y*	*z*	Atom	*x*	*y*	*z*
Molecule A[a]				Molecule B[b]			
Ag(11)	2 340(2)	230(2)	3 368(1)	Ag(21)	4 578(2)	2 506(2)	1 575(1)
Ag(12)	1 895(2)	−1 576(2)	3 538(1)	Ag(22)	6 335(2)	2 946(2)	1 536(1)
Ru(11)	614(2)	−1 206(2)	2 770(1)	Ru(21)	5 837(2)	4 075(2)	2 380(1)
Ru(12)	474(2)	735(2)	2 018(1)	Ru(22)	3 784(2)	4 259(2)	2 984(1)
Ru(13)	363(2)	655(2)	3 127(1)	Ru(23)	4 101(2)	4 429(2)	1 845(1)
Ru(14)	2 345(2)	−256(2)	2 394(1)	Ru(24)	4 859(2)	2 415(2)	2 627(1)
P(11)	2 821(6)	−244(6)	4 277(3)	P(21)	5 156(6)	2 123(6)	655(3)
P(12)	2 526(6)	−2 334(5)	4 390(3)	P(22)	7 218(6)	2 346(6)	690(3)
O(11)	685(17)	−3 353(17)	3 552(10)	O(21)	8 062(24)	3 883(21)	1 808(13)
O(12)	−1 701(21)	−689(18)	2 868(11)	O(22)	5 415(18)	6 406(18)	2 243(10)
O(13)	1 072(18)	−2 047(18)	1 778(11)	O(23)	6 309(20)	3 456(19)	3 541(12)
O(14)	−1 826(17)	1 497(15)	2 108(9)	O(24)	3 149(19)	6 481(20)	3 019(11)
O(15)	676(20)	2 839(21)	1 426(12)	O(25)	1 523(19)	4 302(17)	3 296(10)
O(16)	1 001(25)	183(24)	911(15)	O(26)	3 908(23)	3 570(22)	4 195(14)
O(17)	486(20)	2 841(20)	2 702(11)	O(27)	1 949(19)	4 331(17)	2 016(10)
O(18)	108(17)	581(16)	4 349(10)	O(28)	4 435(16)	4 838(15)	573(9)
O(19)	−1 959(20)	1 471(18)	3 325(11)	O(29)	3 367(20)	6 712(21)	1 715(11)
O(110)	2 714(16)	1 814(16)	1 895(9)	O(210)	2 724(16)	2 184(14)	2 954(8)
O(111)	4 520(16)	−1 395(15)	2 611(8)	O(211)	5 918(17)	236(17)	2 411(9)
O(112)	3 119(18)	−829(18)	1 289(11)	O(212)	5 364(18)	1 440(17)	3 783(11)
C(1)	2 344(22)	−1 369(20)	4 740(12)	C(21)	7 245(26)	3 839(23)	2 015(14)
C(2)	6 294(20)	2 567(20)	274(11)	C(22)	5 499(25)	5 456(26)	2 350(14)
C(11)	673(20)	−2 546(21)	3 299(12)	C(23)	6 099(27)	3 674(26)	3 105(16)
C(12)	−881(31)	−863(26)	2 823(15)	C(24)	3 346(24)	5 608(24)	3 020(13)
C(13)	897(25)	−1 643(25)	2 144(15)	C(25)	2 350(27)	4 293(23)	3 190(14)
C(14)	−910(25)	1 215(23)	2 045(13)	C(26)	4 080(36)	3 790(35)	3 692(22)
C(15)	667(25)	2 008(26)	1 633(15)	C(27)	2 783(26)	4 328(23)	1 983(13)
C(16)	838(32)	260(31)	1 364(20)	C(28)	4 404(23)	4 588(22)	1 060(14)
C(17)	452(26)	1 978(27)	2 851(15)	C(29)	3 642(24)	5 824(25)	1 783(13)
C(18)	313(23)	566(23)	3 871(14)	C(210)	3 537(23)	2 309(21)	2 827(12)
C(19)	−1 050(28)	1 151(25)	3 223(14)	C(211)	5 516(22)	1 111(22)	2 436(12)
C(110)	2 589(20)	1 041(20)	2 078(11)	C(212)	5 159(24)	1 852(23)	3 343(14)
C(111)	3 655(24)	−976(22)	2 573(13)	C(2A1)	4 236(14)	2 859(13)	202(8)
C(112)	2 779(15)	−615(23)	1 727(14)	C(2A2)	3 181(14)	3 128(13)	464(8)
C(1A1)	2 217(15)	745(13)	4 692(9)	C(2A3)	2 425(14)	3 752(13)	146(8)
C(1A2)	1 800(15)	532(13)	5 268(9)	C(2A4)	2 723(14)	4 107(13)	−434(8)
C(1A3)	1 260(15)	1 347(13)	5 534(9)	C(2A5)	3 778(14)	3 837(13)	−696(8)
C(1A4)	1 137(15)	2 376(13)	5 224(9)	C(2A6)	4 534(14)	3 213(13)	−378(8)
C(1A5)	1 554(15)	2 589(13)	4 648(9)	C(2B1)	5 560(15)	755(12)	636(9)
C(1A6)	2 094(15)	1 774(13)	4 382(9)	C(2B2)	5 498(15)	−20(12)	1 134(9)
C(1B1)	4 196(11)	−711(13)	4 284(8)	C(2B3)	5 897(15)	−1 066(12)	1 118(9)
C(1B2)	4 879(11)	−902(13)	3 782(8)	C(2B4)	6 357(15)	−1 338(12)	605(9)
C(1B3)	5 954(11)	−1 301(13)	3 754(8)	C(2B5)	6 419(15)	−563(12)	108(9)
C(1B4)	6 347(11)	−1 509(13)	4 228(8)	C(2B6)	6 020(15)	484(12)	123(9)
C(1B5)	5 665(11)	−1 318(13)	4 729(8)	C(2C1)	8 209(16)	2 937(16)	204(9)
C(1B6)	4 589(11)	−919(13)	4 757(8)	C(2C2)	8 171(16)	3 453(16)	−356(9)
C(1C1)	3 907(11)	−3 077(13)	4 333(8)	C(2C3)	8 936(16)	3 915(16)	−691(9)
C(1C2)	4 398(11)	−3 428(13)	4 786(8)	C(2C4)	9 740(16)	3 860(16)	−467(9)
C(1C3)	5 460(11)	−3 989(13)	4 720(8)	C(2C5)	9 778(16)	3 344(16)	93(9)
C(1C4)	6 030(11)	−4 200(13)	4 202(8)	C(2C6)	9 013(16)	2 882(16)	428(9)
C(1C5)	5 539(11)	−3 850(13)	3 750(8)	C(2D1)	7 909(15)	974(11)	794(8)
C(1C6)	4 478(11)	−3 288(13)	3 816(8)	C(2D2)	7 866(15)	355(11)	1 342(8)
C(1D1)	1 891(15)	−3 241(13)	4 918(8)	C(2D3)	8 363(15)	−718(11)	1 438(8)
C(1D2)	1 953(15)	−4 096(13)	4 749(8)	C(2D4)	8 901(15)	−1 172(11)	985(8)
C(1D3)	1 482(15)	−4 833(13)	5 119(8)	C(2D5)	8 943(15)	−553(11)	437(8)
C(1D4)	949(15)	−4 716(13)	5 658(8)	C(2D6)	8 447(15)	520(11)	342(8)
C(1D5)	887(15)	−3 861(13)	5 827(8)				
C(1D6)	1 358(15)	−3 123(13)	5 457(8)				

[a] Phenyl rings '1A' and '1B' are attached to P(11), and '1C' and '1D' to P(12). Each ring is numbered in cyclic order from the α-carbon. [b] Phenyl rings of molecule B are similarly labelled to those of A (the first digit of each number is changed from 1 to 2).

$^{109}Ag\text{-}\{^1H\}$ INEPT and $^{31}P\text{-}\{^1H\}$ n.m.r. spectra are in excellent agreement (Table 2).

Thus, the $^{109}Ag\text{-}\{^1H\}$ INEPT n.m.r. studies on the clusters (**1**), (**2**), and (**4**) directly confirm that, at ambient temperature in solution, these species undergo a fluxional process which exchanges the silver atoms between the two distinct coinage metal sites in the ground-state structures. These results provide the first direct evidence that the metal skeletons of heteronuclear clusters containing two or more Group 1B metals can exhibit stereochemical non-rigidity in solution.

To the best of our knowledge, the only silver–silver coupling constant which has been previously reported[22] is a value of 35 Hz for $^3J(AgAg)_{av.}$ through a phosphorus–phosphorus double bond in the silver diphosphine complex *trans*-$[Ag(R)P{=}P(R)Ag][SO_3CF_3]_2$ (R = 2,4,6-$Bu^t_3C_6H_2$). Herein we report the first measurement of values of $^1J(^{107,109}Ag^{107,109}Ag)$ (Table 2). Interestingly, even allowing for the low γ value of silver, the magnitudes of these coupling constants (30.4—48.4 Hz) are relatively small compared to typical values of $^1J(^{195}Pt^{195}Pt)$, which are often several thousand Hz.[5] In addition, the values of $^1J(^{107,109}Ag^{107,109}Ag)$ tend to become larger with the increasing number of methylene groups in the backbones of the diphosphine ligands attached to the clusters.

An alternative to the use of the INEPT pulse sequence for obtaining the ^{109}Ag n.m.r. spectra would have been the DEPT experiment,[23,24] which has the advantage that, in the absence of proton decoupling, the multiplets obtained are essentially free of distortion of the relative intensities. However, the time intervals in DEPT are twice those needed for INEPT. With relatively small ^{109}Ag–^1H couplings, this can lead to significant loss of magnetization, as a result of transverse relaxation during the precessional periods, and the resulting DEPT spectra have a poorer signal-to-noise ratio. This effect is illustrated by Figures 5 and 6, which show ^{109}Ag INEPT and DEPT spectra for the simpler system provided by $[AgRu_4(\mu_3\text{-}H)_3(CO)_{12}(PPh_3)]$ (**8**).[11] Table 3 gives the chemical shifts and coupling constants measured in these experiments. The spectra were recorded at −30 °C to prevent the intermolecular exchange of PPh_3 groups between clusters, which was observed at ambient temperature.[11]

The relative simplicity of the spectra of (**8**) also made it possible to conduct a series of ^1H-$\{^{31}P\}$ and ^{31}P-$\{^{109}Ag\}$ selective multiple-resonance experiments, which gave the relative signs of the ^{31}P–^1H, ^{109}Ag–^1H, and ^{109}Ag–^{31}P coupling constants (Table 3). The first of these is illustrated in Figure 7 and shows that $^1J(^{109}Ag$–$^1H)$ and $^1J(^{109}Ag$–$^{31}P)$ are of the same sign, presumably negative. [Note that $\gamma(^{109}Ag) < 0$ and therefore $^1K(^{109}Ag$–$^1H)$ and $^1K(^{109}Ag$–$^{31}P)$ will be positive.] The ^{31}P-$\{^{109}Ag\}$ experiments were also conducted with the phenyl protons selectively decoupled to simplify the ^{31}P spectra and showed that $^1K(^{109}Ag$–$^1H)$ and $^2K(^{31}P$–$^1H)$ are of like sign, so that $^2K(^{31}P$–$^1H)$ [and hence $^2J(^{31}P$–$^1H)$] is also positive.*

Experimental

The clusters (**1**)—(**6**) and (**8**) were synthesized by published methods.[2,11]

Crystal-structure Determination of (**1**).—Suitable crystals of (**1**) were grown from dichloromethane–light petroleum (b.p. 40—60 °C) by slow layer diffusion at −20 °C.

Crystal data. $C_{37}H_{24}Ag_2O_{12}P_2Ru_4$, M = 1 342.6, triclinic, space group $P\bar{1}$ (no. 2), a = 14.159(4), b = 14.317(5), c = 25.828(10) Å, α = 70.59(3), β = 71.98(3), γ = 67.59(2)°, U = 4 464 Å^3, Z = 4, D_c = 1.998 g cm^{-3}, $F(000)$ = 2 568, μ(Mo-K_α) = 21.0 cm^{-1}, crystal size 0.28 × 0.15 × 0.08 mm.

Data collection. Unit-cell parameters and intensity data were obtained by following previously detailed procedures,[25] using a CAD4 diffractometer operating in the ω–2θ scan mode, with graphite-monochromated Mo-K_α radiation. A total of 9 581 unique reflections were collected in the range $3 \leqslant 2\theta \leqslant 42°$. The segment of reciprocal space scanned was: h 0—14, k −14—14, l −26—26. The reflection intensities were corrected for absorption, using the azimuthal-scan method;[26] maximum transmission factor 0.99, minimum value 0.75.

* Reduced coupling constant, $K_{AB} = 4\pi^2 J_{AB}/h\gamma_A\gamma_B$.

Structure solution and refinement. The structure was solved by the application of routine heavy-atom methods (SHELX 86[27]), and refined by full-matrix least squares (SHELX 76[28]).

The asymmetric unit contains two independent molecules and some solvent (disordered CH_2Cl_2, a few atoms for which were included in the final model). Atoms of the type Ru, Ag, and P were refined anisotropically and all hydrogen atoms placed into calculated positions (C–H 0.96, Ag–H 1.72, Ru–H 1.80 Å; U = 0.10 Å^2). The final residuals R and R' were 0.065 and 0.062, respectively, for the 462 variables and 5 515 data for which $F_o > 6\sigma(F_o)$. The function minimized was $\Sigma_w(|F_o| - |F_c|)^2$ with the weight, w, being defined as $1/[\sigma^2(F_o) + 0.000\,05F_o^2]$. Atomic scattering factors and anomalous scattering parameters were taken from refs. 29 and 30, respectively. All computations were made on a DEC VAX-11/750 computer. Atomic co-ordinates are given in Table 4. Additional material available from the the Cambridge Crystallographic Data Centre comprises H-atom co-ordinates, thermal parameters, and remaining bond distances and angles.

N.M.R. Experiments.—^{109}Ag INEPT and DEPT n.m.r. spectra were obtained on a JEOL FX90Q Fourier-transform spectrometer, operating at 4.17 MHz. The ^{109}Ag 90° and 180° pulse lengths were 85 and 170 μs, respectively, and the proton 90° and 180° pulse lengths were 44 and 88 μs, respectively. The ^1H-$\{^{31}P\}$ selective decoupling experiments were also performed on this instrument at an observing frequency of 89.6 MHz. Power at the ^{31}P frequency of 36.2 MHz was transmitted to the proton decoupler coils *via* a tuned amplifier and r.f. matching network. The ^{31}P-$\{^{109}Ag\}$ experiments were performed as described elsewhere on a JEOL FX60 instrument at an operating frequency of 24.2 MHz.[31]

Acknowledgements

We thank the S.E.R.C. for a studentship (to S. S. D. B.) and for an allocation of time on their *X*-ray crystallographic service at Queen Mary College, Johnson Matthey Ltd. for a generous loan of ruthenium and silver salts, the University of Exeter Research Fund Committee for support, Mr. R. J. Lovell for technical assistance, and Mrs. L. J. Salter for drawing the diagrams.

References

1 Part 8, P. J. McCarthy, I. D. Salter, and V. Šik, *J. Organomet. Chem.*, in the press.
2 S. S. D. Brown, I. D. Salter, and L. Toupet, *J. Chem. Soc., Dalton Trans.*, 1988, 757.
3 M. J. Freeman, A. G. Orpen, and I. D. Salter, *J. Chem. Soc., Dalton Trans.*, 1987, 379.
4 I. D. Salter, *Adv. Dynamic Stereochem.*, in the press and refs. therein.
5 R. G. Kidd and R. J. Goodfellow, in 'NMR and the Periodic Table,' eds. R. K. Harris and B. E. Mann, Academic Press, London, 1978, ch. 8.
6 G. A. Morris and R. Freeman, *J. Am. Chem. Soc.*, 1979, **101**, 760.
7 D. P. Burum and R. R. Ernst, *J. Magn. Reson.*, 1980, **39**, 163.
8 See, for example, G. C. van Stein, G. van Koten, K. Vrieze, A. L. Spek, E. A. Klop, and C. Brevard, *Inorg. Chem.*, 1985, **24**, 1367 and refs. therein.
9 S. S. D. Brown, I. J. Colquhoun, W. McFarlane, M. Murray, I. D. Salter, and V. Šik, *J. Chem. Soc., Chem. Commun.*, 1986, 53.
10 P. A. Bates, S. S. D. Brown, A. J. Dent, M. B. Hursthouse, G. F. M. Kitchen, A. G. Orpen, I. D. Salter, and V. Šik, *J. Chem. Soc., Chem. Commun.*, 1986, 600.
11 R. A. Brice, S. C. Pearse, I. D. Salter, and K. Henrick, *J. Chem. Soc., Dalton Trans.*, 1986, 2181.
12 J. S. Bradley, R. L. Pruett, E. Hill, G. B. Ansell, M. E. Leonowicz, and M. A. Modrick, *Organometallics*, 1982, **1**, 748.
13 B. F. G. Johnson, J. Lewis, W. J. H. Nelson, M. D. Vargas, D. Braga, K. Henrick, and M. McPartlin, *J. Chem. Soc., Dalton Trans.*, 1986, 975.

14 S. S. D. Brown, S. Hudson, I. D. Salter, and M. McPartlin, *J. Chem. Soc., Dalton Trans.*, 1987, 1967.
15 L. J. Farrugia, M. J. Freeman, M. Green, A. G. Orpen, F. G. A. Stone, and I. D. Salter, *J. Organomet. Chem.*, 1983, **249**, 273.
16 L. W. Bateman, M. Green, K. A. Mead, R. M. Mills, I. D. Salter, F. G. A. Stone, and P. Woodward, *J. Chem. Soc., Dalton Trans.*, 1983, 2599.
17 J. A. Iggo, M. J. Mays, P. R. Raithby, and K. Henrick, *J. Chem. Soc., Dalton Trans.*, 1984, 633.
18 B. F. G. Johnson, D. A. Kaner, J. Lewis, P. R. Raithby, and M. J. Taylor, *J. Chem. Soc., Chem. Commun.*, 1982, 314.
19 P. Braunstein, J. Rosé, A. Dedieu, Y. Dusausoy, J-P. Mangeot, A. Tiripicchio, and M. Tiripicchio-Camellini, *J. Chem. Soc., Dalton Trans.*, 1986, 225.
20 M. Ahlgren, T. T. Pakkanen, and I. Tahvanainen, *J. Organomet. Chem.*, 1987, **323**, 91.
21 R. Benn and H. Günther, *Angew. Chem., Int. Ed. Engl.*, 1983, **22**, 350.
22 A. H. Cowley, N. C. Norman, and M. Pakulski, *J. Chem. Soc., Chem. Commun.*, 1984, 1054.
23 D. M. Doddrell and D. T. Pegg, *J. Am. Chem. Soc.*, 1980, **102**, 6388.
24 D. M. Doddrell, D. T. Pegg, and M. R. Bendall, *J. Magn. Reson.*, 1982, **48**, 323.
25 M. B. Hursthouse, R. A. Jones, K. M. A. Malik, and G. Wilkinson, *J. Am. Chem. Soc.*, 1979, **101**, 4128.
26 A. C. T. North, D. C. Phillips, and F. S. Mathews, *Acta Crystallogr., Sect. A*, 1968, **24**, 351.
27 G. M. Sheldrick, SHELX 86, Program for Crystal Structure Solution, University of Göttingen, 1986.
28 G. M. Sheldrick, SHELX 76, Program for Crystal Structure Determination and Refinement, University of Cambridge, 1976.
29 D. T. Cromer and J. B. Mann, *Acta Crystallogr., Sect. A*, 1968, **24**, 321.
30 D. T. Cromer and D. Liberman, *J. Chem. Phys.*, 1970, **53**, 1891.
31 I. J. Colquhoun and W. McFarlane, *J. Chem. Soc., Chem. Commun.*, 1980, 145.

Received 5*th October* 1987; *Paper* 7/1777